Nuclear lipidome is altered in amyotrophic lateral sclerosis: a preliminary study

Omar Ramírez-Nuñez[a,1], Mariona Jové [a,1], Pascual Torres [a1], Joaquim Sol[a], Laia Fontdevila [a], Ricardo Romero-Guevara[a], Victòria Ayala[a], Chiara Rossi[a], Jordi Boada[a], Mònica Povedano[b], Pol Andrés-Benito [c,d] , Isidro Ferrer [c,d], Reinald Pamplona [a], Manuel Portero-Otin[a,2]

OR-N:omar.ramirez78@gmail.com; MJ:mariona.jove@mex.udl.cat; PT:pascual.torres@mex.udl.cat; JS:solcullere@gmail.com;LF:laia_fontdevila@hotmail.com; RR-G:rromeroguevara@gmail.com; VA:victoria.ayala@mex.udl.cat;CR: clara70289@mex.udl.cat; JB:Jordi.boada@mex.udl.cat;RP: Reinald.pamplona@mex.udl.cat

[a]Department of Experimental Medicine, School of Medicine, IRBLleida-UdL, Avda Rovira Roure 80 25196, Lleida, Spain

MP: 30058mpp@gmail.com

[b]Neurology Service, Hospital Universitari de Bellvitge, L'Hospitalet de Llobregat, c/La Feixa Llarga, S/N 08908 Hospitalet de Llobregat, Barcelona, Spain

PA-B:pol.andres.benito@gmail.com; IF:8082ifa@gmail.com

[c] Departament of Pathology and Experimental Therapeutics, Universitat de Barcelona; Hospital Universitari de Bellvitge, IDIBELL, Hospitalet de Llobregat;

[d] CIBERNED (Centro de Investigación Biomédica en Red de Enfermedades Neurodegenerativas), Instituto Carlos III, c/La Feixa Llarga sn, 08908 Hospitalet de Llobregat, Barcelona, Spain

[1]These authors contributed equally to this work

[2]To whom correspondence should be addressed at IRBLleida-UdL, Edifici Biomedicina I, Avda Rovira Roure 80 E25196 Lleida, Spain. Phone +34973702408; Fax: +34973702426; e-mail: manuel.portero@mex.udl.cat

ABSTRACT

In this pilot study, we show that nuclei in spinal cord from ALS patients exhibit a differential lipidomic signature. Among the differential lipid species we could annotate 41 potential identities. These comprise membrane-bound lipids such as phosphatidylethanolamines –including plasmalogens- and phosphatidylcholines but also other lipid classes such as glycosphingolipids, diacylglycerols, and triacylglycerides (potentially present

as nuclear lipid droplets). These results were orthogonally validated by showing loss of alkyldihydroxyacetonephosphate synthase (AGPS), a key peroxisomal enzyme in plasmalogen synthesis, both in ALS necropsy samples, in human motor neurons derived from iPSC from ALS patients and in hSOD-G93A transgenic mice. Further, diacylglycerol content changes were associated to ALS-linked variations in related-enzymes, such as phospholipase C ßI (PLCßI), the source of nuclear diacylglycerol, and protein kinase CßII (PKCßII), whose function partially depends on nuclei concentration of diacylglycerol. These results point out for not only a role of nuclear membrane lipids but also to lipids present in the nucleoplasm, suggesting an undisclosed role for this part of the subcellular lipidome in ALS pathophysiology.

Keywords

Motor neuron; lipidomic; nuclear envelope; polyunsaturated fatty acids; subcellular lipidomics; phospholipase C ßI; protein kinase CßII; alkyldihydroxyacetonephosphate synthase

INTRODUCTION

Amyotrophic lateral sclerosis (ALS) is a devastating neurodegenerative disease, where patients exhibit a loss in motor neuron number. This cell demise has been associated to a number of cellular events common to other age-related neurodegenerative conditions. These include the accumulation of modified proteins, such as Tar-DNA binding of 43 kDa (TDP-43) and ERK, in non-physiological subcellular locations [1]. Interestingly, these proteins play essential roles in nucleus, so their presence out of nucleus might be a consequence of an impairment in normal nucleocytosolic traffic. Indeed, it is known that this physiological trait is affected in ALS[2]. Nucleocytosolic transport depends on a series of proteins such as Ran-GTPases as well as the nuclear pores function. Of note, these nuclear pores are embedded into the nuclear envelope lipid bilayers. Further, recent data demonstrate alterations in nuclear membrane in ALS models [3]

Lipids are key players in cellular physiology. Lipid composition is an essential feature of neural tissue. Recent data from our group and others have revealed that in ALS an extensive array of changes involving tissue lipidome is present. Indeed, in experimental models of ALS, dietary changes in lipid composition induce changes in phenotype of this neurodegenerative condition. Furthermore, epidemiological data demonstrate that the dietary intake of selected lipids (such as those belonging to n-3 family) is a relevant factor in predicting the incidence of this condition[4].

To the date, the lipidome of nuclear envelopes has been focus of relative attention in some conditions [5]. However, whether it is affected in ALS is currently unknown. To shed light into this question, we designed a pilot study to analyze samples from spinal cord of ALS patients, and age and gender matched individuals, to explore if ALS is associated to changes in nuclear lipidome(s). This has been achieved after nuclei enrichment from frozen tissues after necropsy and subsequent lipid analyses by liquid chromatography coupled to time-of-flight mass spectrometry. The results reveal an important change not only in typical membrane lipids but also affecting signaling molecules. The suggested pathogenic pathways have been validated independently by evaluating the levels and distribution of key proteins related with differential lipids, both in human samples and in a transgenic mice model overexpressing an ALS-related gene.

METHODS

Human and mice neuronal tissues

All human samples were obtained from the Institute of Neuropathology and HUB-ICO-IDIBELL Brain Bank following the guidelines of the local ethics committees. Extensive pathological studies were done for ALS diagnosis as previously described[6]. Samples lumbar spinal cord were from 2 males and 2 females aged between 57 and 79 years affected with typical neurological and neuropathological characteristics of sporadic ALS. The post-mortem delay between death and tissue processing was between 3 and 16h. Age- and gender-matched controls with no clinical evidences of neurological disease and with a normal neuropathological study were processed in parallel (see Table 1).

We also employed lumbar spinal cord samples from male mice (150 d, n=5) from the strain B6SJL-Tg (SOD1-G93A)1Gur/J (from now on G93A) purchased at The Jackson Laboratories (JAX catalogue stock number 002726, Bar Harbor, MN, USA) and maintained in the B6SJL background, by male founder crossing with B6SJLF1/J. As controls we employed non-transgenic littermates. Mice care and housing have been previously described [7]. Animals, after being fasted overnight, were anaesthetized with 2.5% isoflurane in air and finally sacrificed. Spinal cords were rapidly excised, frozen in liquid N_2 and stored at -80ºC until further analyses.

For western-blot, samples were homogenized on ice in a buffer containing 180 mM KCl, 5 mM MOPS, 2 mM EDTA, 1mM diethylenetriaminepentaacetic acid, and 1 µM of freshly prepared butylated hydroxyl toluene at pH 7.3 using a homogenizer device (T10 basic UltraTurraX, IKA, Staufen, Germany). Protein concentrations were measured by the Bradford method. For immunohistochemistry, animals after sacrifice were exanguinated by perfusion, firstly with saline solution (4ºC) and thereafter with ice cold 0.4% paraformaldeyde (Sigma-Aldrich, Sant Louis, MO, USA) solution (freshly prepared with pH 7.4 phosphate buffer). All experimental procedures were approved by the Institutional Animal Care Committee of IRBLleida and were conformed to the Directive 2010/63/EU of the European Parliament.

Human Induced pluripotent stem (hIPS)cell-derived motor neurons

hiPS were obtained from NINDS Human Genetics DNA and Cell line Repository at Coriell Institute (Camden, NJ, USA #ND35663 –with a mutation in *FUS*-, #ND42765 –with a C9ORF72 expansion-, and #ND41865 –control cell line-) and grown in standard human embryonic stem (ES) cells media supplemented with 6ng/ml basic Fibroblast Growth Factor (bFGF) on inactivated mouse embryonic fibroblast (MEFs) (Sigma) as feeder cells. Differentiation towards motor neurons was carried by a modification of Du et al protocol[8]. Briefly, undifferentiated hiPSC cultures were digested with Accutase solution (Sigma-Aldrich) for 5 min, seed for 40 min in MEFs-conditioned hES media plus 10µM Y27632 (Cayman Chemicals, Ann-Arbor, MI, USA) to remove as many fibroblasts as possible, then the cell suspension was transferred into Geltrex®(Thermo Scientific)-coated tissue culture dishes for 24-48hrs until stem colonies were visible. Media was then changed to neuroepithelial media (NEPM) for 6 days, and then replaced sequentially to motorneuron progenitor (MNPs) media 1st and 2nd , 6 days in each of them. At this point, progenitors were either expanded on MNPs 2nd or further differentiated into neurospheres and motor neurons using motor neuron induction media and motor neuron maturation media respectively. Importantly, for neurosphere formation non-tissue culture dishes without coating were used. Both neuroepithelial and MNPs were split into new Geltrex®-coated dishes when 70-100% confluent and seed at 50-75 000 cells/cm² and always using Y27632 10µM during the 1st 24 hrs. Media was changed every other day.

After 6 days in motor neuron induction media, neurospheres were collected in a15 ml centrifuge tube, spin down 3.5 min at 0.1rcf , supernatant discarded and spheres digested for 5-7 min in Accumax solution (Sigma). With the help of a pipette, cells clusters were disaggregated until an homegenous single cell suspension was obtained. Cells were then washed with DMEM/F12 (Thermo Scientific) and resuspended in motor neuron

maturation media for seeding, media was supplemented with Y27632, Laminin (2.5 µg per 1ml of media, Thermo-Fisher) and 0.1µM Compound-E (Stem Cell Technologies, Grenoble, France) during the first 3 days after plating in Poly-L-Lysine (Sigma) coated dishes, media change was done every 72 hrs. Seeding density was maintained at 50-100 000 cells/cm². The different media composition appears in the Table 2.

Nuclear enrichment

Nuclei were extracted from portions of the human spinal cord according to a variation of the Blobber and Potter protocol [9]. We started from about 0.270 g of frozen tissue, which was allowed to thaw at 4 °C. All subsequent steps, unless noted otherwise, were performed at this temperature. Once thawed, samples were cut into very small pieces with a scalpel and transferred to a 2 mL eppendorff, where the tissue was homogenized in two volumes (w/v) of 0.25 M sucrose in cold TKM (0.05 M Tris, 0.025 M KCl. MgCl2 0.005 M) and commercial protease and phosphatase inhibitors (78440, Thermo Scientific). The homogenization was first performed with a Polytron® mechanical homogenizer with a plastic plunger with approximately 20-40 strokes. The homogenate was then passed to a Dounce-type homogenizer with a glass tight plunger (20-40 strokes). At the end of this step, the homogenate (540 µL) was transferred to an ultracentrifuge tube (Beckman Coulter, 344057), and 1080 µL of 2.3 M sucrose in TKM were added, with the contents of the tube were carefully mixed by inversion. A pipette was then introduced to the bottom of the centrifuge tube and 540 µL of 2.3 M sucrose in TKM were carefully added, ensuring that well-defined phases of sucrose were formed, where the homogenate remained at the top. The ultracentrifuge tubes were centrifuged at 124000 x g at 4 ° C for 30 minutes in Optima L-100XP ultracentrifuge (Beckman Coulter, SW 55 Ti rotor). The resulting pellet was suspended in 50 µL of TKM with protease inhibitors and commercial phosphatases (78440, Thermo Fisher Scientific). The presence of nuclei was confirmed by fluorescence microscopy, after staining with DAPI at 1 µg/mL. For comparison of nuclear enrichment, mitochondrial enriched fractions were isolated as indicated in Mitochondria Isolation Kit for Tissue (Ab110168, Abcam).

Lipidomics of isolated nuclei

The lipids of the isolated spinal cord nuclei extracted post mortem of ALS patients and controls were extracted using methyl-tert-butyl-ether with the help of a sonicator, after adding deuterated internal standards representing major lipid classes[10]. The analysis was performed using a liquid chromatograph (Agilent 1290 UPLC) coupled to a mass spectrometer (Agilent 6520 ESIQTOF-MS) that allows the characterization of lipids and

metabolites based in the exact mass (<10 ppm), isotopic spectrum and in retention times of internal standards marked isotopically and representative of the major lipid classes. Lipid species were separated through reverse phase chromatography (Waters Acquity HSS T3 × 0.1 mm × 100 mm at 55 ° C), in suitable gradients and previously described [10]. The eluate was monitored in the Q-TOF system by electroespray in positive and negative ionization mode, collecting data in a range of m/z from 100 to 3000, with ionization source at 120ºC and using N2 as a solvation gas at 250 °C (800 L/h). The exact mass adjustment is performed by joint infusion in reference spray of purine and HP9982, with exact masses with errors less than 0.5 ppm. Tandem mass spectrometry was performed as described[10].

After the extraction of the molecular characteristics, the analysis of the results was performed using the Mass Profiler software (Agilent, version for mass spectrometry). All samples were coded and analyzed in double blind mode. After the data collection, they were decoded and the relevant statistical analyses, both univariate and multivariate, by the R package OrbisMet (available in http://hdl.handle.net/10609/65305)

Microscopy of isolated nuclei.

The isolated nuclei were fixed in 4% paraformaldehyde (w/v) in PBS at a 1/3 (nuclei solution/fixation solution) at room temperature for 15 minutes. Subsequently, 20 µL of the mixture were placed on a round coverslip (12 mm), which was subsequently centrifuged (100xG, 3 min). At the end of the time, coverslips were taken with fine forceps and placed on a Parafilm®-covered support. The nuclei were incubated in a permeabilization and blocking solution (Triton X-100 0.1%, normal goat serum 10% in PBS) for 30 minutes at room temperature. Then, three gentle washes were carefully made with PBS. Coverslips were incubated at 4°C overnight (in a humid chamber) with the appropriate primary antibodies at the indicated final concentrations, dissolved in 1/10 (v/v) of blocking solution in PBS. After this incubation period, three washes were made with PBS and the samples were incubated with the appropriate secondary antibody dissolved in PBS and 1 µg / mL DAPI for nuclear staining, at 4 °C for 1 hour. Finally, 3 washes of 5 minutes each were made with PBS and the nuclei were mounted on slides with Fluoromount-G solution (00-4959-52, Thermo Fisher Scientific) and allowed to dry at room temperature. Nile Red at 10µg/mL in PBS was used to evaluate the presence of lipid droplets, by incubating coverslips containing fixed nuclei at 37ºC for 30 min.

Western Blot analysis

In case of human samples, protein from different fractions (total lysates, mitochondrial and nuclei enriched fractions) was extracted using radioimmunoprecipitation buffer with Halt Protease Inhibitor Cocktail (1X) (1861278, Thermo Fisher Scientific). After sonication, protein quantification was performed with Bradford assay. Both for human and mice samples, 15 µg of protein were loaded onto a 12% acrylamide SDS-PAGE gel. Membranes were blocked with I-Block (T2015, Thermo Fisher Scientific) for 1 hour and incubated overnight with the antibodies and conditions listed in Table 2. After primary antibody incubation, membranes were washed 3 times with TBS-T 0.05% and incubated with secondary antibody for 1h. Immobilon™ Western Chemiluminiscent HRP Substrate (Merck Millipore, WBKLS0500, Billerica, MA, USA) was used for immunodetection. Membranes were stained with Coomassie Brilliant Blue G (27815, Sigma-Aldrich) for normalization. Specific bands were quantified with ImageLab v5.2.1 (Bio-Rad). Omission of primary antibody resulted in complete loss of signal.

Immunofluorescence.

Immunofluorescence was performed essentially as previously described [1]. Briefly, after tissue collection (lumbar spinal cord) in mice, samples were immersed for 24h in paraformaldehyde solution to assure preservation. Samples were thereafter immersed in 30% sucrose, (made in pH 7.4 phosphate buffer) for 48h to achieve cryopreservation. Tissue was encased in a cubic recipient (Peel-A-Way Disposable Embeding Molds-S-22, Polysciences Inc., Warrington, PA, USA), labelled and embedded in tissue freezing medium (Triangle Biomedical Sciences Inc., Newcastle, UK) for easy cutting and better preservation and finally frozen (-80ºC). Sixteen µm wide sections of lumbar spinal cord were cut and carefully seeded along gelatin-coated slide. Selected sections were permeabilized with 0.1% Triton X-100 in PBS for 30 min at room temperature. Blocking of sections was performed with 5% normal goat serum in 0.1% Triton X-100 PBS at room temperature for 1h. In the case of human MNs, cells (grown in glass coverslips) were washed with PBS and then fixed with 3.7% paraformaldehyde for 10 min at room temperature. Cells were rinsed with PBS, permeabilised with 0.1% Triton X-100 in PBS for 30 min and subsequently blocked with 5% fetal horse serum at room temperature for 2 hours.

For immunofluorescence, slides (mouse spinal cord sections) or coverslips (human MNs) were incubated at 4 °C overnight with the primary antibodies indicated on table 3. Next day, slides and coverslips were washed with

PBS three times for 5 min at room temperature. Then, they were incubated at room temperature for 1h in darkness with corresponding secondary antibodies. Sections and cells were finally counterstained with 4,6-diamidino-2-phenylindole dihydrochloride (DAPI, 1 ug/ml) in PBS at room temperature for 10 min and, after three washes with PBS, mounted on slides with Vectashield (Vector Laboratories, Burlingame, CA, USA). In selected sections and coverslips, primary antibody was omitted to assure labelling specificity. Mounted slices were examined under a Fluoview 500 Olympus confocal laser scanning microscope (Olympus, Hamburg, Germany). For quantification tissue immunoreactivity images were analyzed with the Image J software (http://rsbweb.nih.gov/ij/) and human MNs images were evaluated using an ad-hoc designed Cell Profiler pipeline (http://cellprofiler.org), available in supplemental materials.

Statistical analyses

All statistics were performed using the Prism software (GraphPad Software, San Diego, CA, USA). Differences between groups were analyzed by the Student's t tests or ANOVA after normality of variable distribution was ensured by Kolmogorov-Smirnov test. The 0.05 level was selected as the point of minimal statistical significance in every comparison

RESULTS

The described method (Figure 1a) leads to a fraction enriched in nuclei, derived from frozen tissues. The nuclei present in this fraction exhibit a preserved nuclear morphology (DAPI positivity with high nucleoporin content –Figure 1b). Further, a high content of nuclear specific proteins was demonstrated by western blot analyses (Figure 1C). The potential presence of membrane containing organelles, such as mitochondria, was excluded, based on the content of mitochondrial membrane markers such as porin or mitofusin (Figure 1c).

Lipidomic analyses disclosed significant differences between nuclei from ALS and age-matched healthy controls. Thus, principal component analyses (PCA) explained more than 50% of total variances (either in negative or in positively ionized lipids) of present samples in a model of three components (Figure 2a). Further, partial-least square models offered an accuracy in predicting the groups *ca* 100%, with more than 60% of total variance in lipidomic profiles being explained in three major components, demonstrating the robustness of the model (Figure 2b). As shown by hierarchical clustering analyses (Figure 2c), marked differences were present among the lipidomic profiles of the resulting nuclei enriched fractions.

Univariate analyses (T test) demonstrated the presence of 151 differential molecules (99 in positive ionization and 52 in negative ionization, Supplemental table 1, p values between 9.46x10E-15 and 0.05). Among these, putative identities, based on isotope distribution pattern and retention time identity with internal standards representative of lipid major families, were found for 41 different molecules (25 upregulated in ALS samples; Table 3), with p values ranging from 5.35x10E-5 to 0.05. Potential identities (comprising isobaric molecules) included 8 ceramides, 9 diacilglycerol, 8 phosphatidylcholines,15 phosphatidylethanolamines, 9 phosphatidic acid, 7 phosphatidylserines, 2 phosphoinositides and 11 triacylglycerides.

After tandem mass spectrometry, we were able to confirm the identity of diacylglycerol molecules (DAG). One of the mediators of DAG is PKCßII. In line with altered levels of DAG, decreased levels of PKCßII were measured in both spinal cord lysates from ALS patients (Figure 3a) and lysates from G93A mice (Figure 3b), in comparison to adequate controls. Further, as DAG can be the result of the activation of an specific PLC isoform (ßI), we measured its levels in the same samples. Though immunoreactivity was near to marginal in human spinal cord lysates, clear decreases could be also measured in G93A spinal cord lysates (Figure 3c and 3d).

Similarly, as differential lipids also comprised several plasmalogens, we explored the potential changes of one of the rate-limiting enzymes for plasmalogen synthesis, AGPS [11], a peroxisomal enzyme. The results indicate that ALS could influence AGPS levels in spinal cord. Thus, western-blot analyses (Figure 4a) demonstrate significantly decreased levels in spinal cords of G93A mice in comparison with non-Tg animals. In contrast, in lysates from human samples, we were not able to reproduce this fact (Figure 4b). Noteworthy, in human motor neurons derived from IPs, the anti-AGPS immunroeactivity in two cell lines from known ALS-causing mutations (*FUS* and C9orf72 expansions) was lower than that from control cell line (Figure 4c). Further, there was a significant correlation between nuclear perimeter and AGPS levels in both control and C9orf72 cell lines, but not in *FUS* mutants. Confirming these data, in mice spinal cord, this protein was preferentially present in motor neurons, whose levels were severely decreased in 150 days old G93A mice (Figure 4d).

Furthermore, some of the potential identities of the differential lipids are alkyl-phospholipids, whose synthesis is also dependent on peroxisome function. To evaluate whether changes in AGPS and in alkyl-phospholipids are due to a potentially specific peroxisomal defect, we evaluated PMP70 distribution in G93A mice. Results

(Figure 5a) show that despite PMP70 enriched vesicles were present in many remaining motor neurons in G93A mice spinal cord, no general increases were evident by western-blot. Since we also detected differential phospholipid compositions in nuclear isolates, we evaluated SCP-2 expression. SCP-2 is a peroxisomal/ER resident protein implicated in phospholipid synthesis[12], particularly phosphatydilethanolamine and phosphatidylserine. In line with differential phospholipids found in nuclei isolated from ALS samples, we found a marked rearrangement of SCP-2 immunoreactivity in G93A mice. As shown in figure 5c, in control mice, SCP-2 expression was preferentially found around the nuclei, this was not the case in many motor neurons from G93A mice, with redistribution on this immunoreactivity towards vesicles with no perinuclear enrichment. Further, levels of SCP-2 were significantly increased, as shown by western-blot analyses.

Finally, across the differential lipids in enriched nuclear fractions we detected molecules compatible with triacylglycerides. As these are usually found in lipid droplets[13], we explored if lipid droplets could be found along the purified nuclei. As shown in figure 6, Nile Red stained vesicles could be found associated with the nuclei and even inside.

DISCUSSION

The analysis of the lipidomic profile of the isolated nuclei of post tissue mortem of ALS patients and controls demonstrate a differential profile between control group and the pathological group. To the best of our knowledge, this is the first report indicating a difference in this subcellular parameter in this devastating neurodegenerative disease. There is not a large number of references on cellular membrane alterations in ALS and their models, although in previous studies of our group [6,7], demonstrate severe changes in tissue lipidomes in ALS and ALS models, depending on disease stage and anatomical location.On the other hand, it should be remembered that one of the forms of familial ALS (subtype 8), is due to a mutation in the VAP-B protein, involved in intracellular membrane trafficking [14]. Thus, it can be expected that the composition of the intracellular membranes is a relevant factor in pathophysiology of ALS.

Specifically about the nuclear envelope, it has been recently described that failures in nucleocytosolic transport, depending in part from importins, are present in ALS [15]. The interaction between the lipids of the nuclear membranes and the nucleoporins –integral components of nuclear pore- as well as their contribution to cellular homeostasis is a field largely unknown. To perform their function, nucleoporins need to be anchored adequately

at the fusion points between the nuclear membranes of external and internal nuclear envelope[16]. There are highly specialized regions of specific nucleoporins (such as Pom121, GP201) structurally dependent on phospholipids where these proteins are anchored into [17,18]. In addition to these transmembrane proteins, other proteins, such as members of the NUP107-160 complex contain domains that interact with the nuclear membranes[19,20]. Our results are compatible with changes in the composition of the membranes that make up the nuclear envelope, since phospholipids involved include phosphatidylethanolamine, phosphatidylcholine and phosphatidylinositol, all membrane components. Noteworthy, it shall be reminded that nuclear envelop leaflets are in continuity with endoplasmic reticulum membranes. Therefore, changes in nuclear envelope can be related with dysfunctions in this membranous organelle, already characterized in ALS[3,6,21]

DAG in nucleus has a signaling role, reviewed in [21], and it is derived from the activity of a PLCß1 isoform. In line with altered homeostasis of nuclear DAG in ALS, we detected different amounts of PLCß1 in tissue lysates from G93A mice and potentially from ALS patients. This enzyme is present in neuronal cells in rat brain [22], partially present in nuclei. Further, it is known that this enzyme is sensitive to endoplasmic reticulum stress[23], a well described pathogenic mediator in ALS[6]. Interestingly, a loss in PLCß1 has been also described in other neurodegenerative conditions linked to protein aggregation, such as Pick's disease [24] and Creutzfeld-Jacobs disease[25]. Furthermore, PLCß1 loss induces an age-dependent loss of neurites and neurodegeneration[26]. Nonetheless, it is known that metabotropic glutamate receptors regulate synaptic transmission through the stimulation of PLCß1 [27]. Of note, activation of metabotropic signaling has been proposed as novel potentially therapeutic strategy in ALS[28]. DAG build-up in nucleus leads to PKCßII nuclear translocation[21]. For this reason, we evaluated whether, in line with altered DAG and PLCß1 levels in ALS, this disease is associated with changes in PKCßII. The results indicate that, both in ALS patients and in G93A mice, PKCßII levels are diminished. Up to date, no previous evidence of its involvement in this disease were known, except with the fact that PKC levels were increased in ALS patients [29]. The involvement of the potential loss of PKCßII in ALS pathogenesis can be diverse, as this protein interacts with mitochondria[30], and with autophagic function[31], to name a few, and both elements are involved in ALS [32,33]

Other changes in lipid components of nuclei include plasmalogens. These membrane glycerophospholipids contain a fatty alcohol with a vinyl-ether bond at the sn-1 position, and they are enriched in polyunsaturated fatty acids at the sn-2 position of the glycerol backbone. For this reason, they have been involved in the redox

homeostasis of membranes[34], and its Previous data have characterized plasmalogens in the nuclear envelope of postmytotic tissues such as myocardium [35]. Peroxisomes contribute to plasmalogen synthesis, and previous data of our group describe alterations in peroxisomal enzymes in ALS tissues [36]. Whether the loss of plasmalogen present in ALS nuclei is potentially derived from this peroxisomal disturbance and whether it contributes to ALS pathophysiology is still unknown. Nonetheless, AGPS intensity was strongly diminished in G93A mice motor neurons, supporting a potential involvement of this pathway in the pathophysiology of the spinal cord dysfunction present in these mice.

Among differential lipids, other classes are also present. These include triacylglycerides, which could be explained by changes in the so-called lipid droplets, recently described in the nucleoplasm[37] where it may derive from inner nuclear membrane[38]. Since lipid droplet physiological role in nuclei is mainly unknown, we cannot infer its pathophysiological significance in our samples. Nonetheless, recent data disclose that glial cells accumulate lipid droplets as a response to excitotoxicity[39]. However, they may also play a role in neurodegeneration in lipid peroxidation-prone environments[40] . Our finding that no general effect (not all triaclyglycerides increase or decrease) is present, may be derived from potentially heterogeneous cellular source of the nuclei.

Similarly, another group of lipids with potential relevance are sphingolipids. Previous findings in the field suggest the importance of these lipids in ALS. In the G93A model, alterations are demonstrated in tissue levels during the development of the disease. Further, the administration of GM3, one of its members, leads to an improvement in the clinical course of the disease [41]. In a close relationship, it has been also shown that the transcription of glucosylceramide synthase is necessary for optimal protection against denervation, and that its inhibition worsens the clinical course in another model of the family ALS, the mouse hSODG86R [42] . Our results are fully compatible with these data, as we found significantly decreased levels of two molecules compatible with glucosylceramide identity. As these molecules are functionally involved in cell signaling, autophagy and determination of lipid membrane functional domains [43,44], its potential role in ALS pathophysiology merits further investigation.

We acknowledge, as a limitation of our work, the low number of individuals used. However, even with such a limitation, the profiling of a high number of nuclei is possible, and allows to distinction of clear lipidomic

profiles. Further, the high heterogeneity of nuclear structures does not permit to attribute these changes to a specific cell subtype. Similarly, we do not know if freezing procedures have led to a selective enrichment of given cellular types or nuclei. Thus, we cannot exclude that specific nuclei can be more resistant to postmortem changes and criopreservation. However, we assume the fact that nuclei enrichment is robust, based on the absence of mitochondrial markers –major contaminants in similar procedures-, and the morphological and biochemical evidences for nuclear presence. Despite these limitations, changes in two lipid families (plasmalogen and DAG) were independently validated by exploring their potential molecular basis. We think that the combination of the described technologies (lipidomic analyses applied to subcellular fractionation of pathologically relevant samples) could pave the way for the discovery of novel biomarkers and pathophysiologically relevant pathways.

DECLARATIONS

Ethics approval and consent to participate

Samples from human individuals were obtained from the Institute of Neuropathology and HUB-ICO-IDIBELL Brain Bank following the guidelines of the local ethics committees. Experiments with mice were approved Institutional Animal Care Committee of IRBLleida and were conformed to the Directive 2010/63/EU of the European Parliament.

Consent for publication

Not aplicable

Availability of data and material

The Orbismet, the R package employed for analyses of lipidomic data during the current study are available in the UOC repository, at in http://hdl.handle.net/10609/65305

Competing interests

The authors declare that they have no competing interests

Funding

This work was supported by the Seventh Framework Programme of the European Commission, [grant agreement 278486: DEVELAGE to IF]; by the the Autonomous Goverment of Catalunya [2017SGR696] and the Spanish Ministry of Health [PI14/1115, 14/003218 PI17-00134]; and the "Marató de TV3" Foundation (PP00111). MJ is a Serra Hunter program fellow. RRG is a fellow from Marie Curie Cofund IRBLleida-IPP (EU 7th Framework Program, 609396 agreement). PT is a predoctoral fellow from Spanish Ministry of

Education [FPU16/01446]. LF, CR and OR-N are predoctoral fellows from the Autonomous Government of Catalonia. Supported also by a FUNDELA Grant, RedELA-Plataforma Investigación and the Fundació Miquel Valls (Jack Van den Hoek donation). FEDER funds are acknowledged ("A way to make Europe")

Authors' contributions

OR-N,MJ and PT optimized the nuclei isolation, and performed western-blot analyses. MJ and JS performed lipidomic data, designed R packages and analyzed these data. RR-G,PA-B, LF and CR generated transgenic mice, maintained iPSc and characterized motor neurons and derived results. VA,MP and JB performed general data analyses. RP, IF and MP-O planned the experiments, curated data, drafted the manuscript and prepared figures. All authors read and approved the final manuscript.

Acknowledgements

We are indebted to tissue donors and their families.

REFERENCES

Bibliography

1. Ayala V, Granado-Serrano AB, Cacabelos D, Naudí A, Ilieva EV, Boada J, Caraballo-Miralles V, Lladó J, Ferrer I, Pamplona R, et al. (2011) Cell stress induces TDP-43 pathological changes associated with ERK1/2 dysfunction: implications in ALS. *Acta Neuropathol* **122**: 259–270.
2. Chou C-C, Zhang Y, Umoh ME, Vaughan SW, Lorenzini I, Liu F, Sayegh M, Donlin-Asp PG, Chen YH, Duong DM, et al. (2018) TDP-43 pathology disrupts nuclear pore complexes and nucleocytoplasmic transport in ALS/FTD. *Nat Neurosci* **21**: 228–239.
3. Gautam M, Jara JH, Kocak N, Rylaarsdam LE, Kim KD, Bigio EH, Hande Özdinler P (2018) Mitochondria, ER, and nuclear membrane defects reveal early mechanisms for upper motor neuron vulnerability with respect to TDP-43 pathology. *Acta Neuropathol*.
4. Fitzgerald KC, O'Reilly ÉJ, Falcone GJ, McCullough ML, Park Y, Kolonel LN, Ascherio A (2014) Dietary ω-3 polyunsaturated fatty acid intake and risk for amyotrophic lateral sclerosis. *JAMA Neurol* **71**: 1102–1110.
5. Farooqui AA, Ong W-Y, Farooqui T (2010) Lipid mediators in the nucleus: Their potential contribution to Alzheimer's disease. *Biochim Biophys Acta* **1801**: 906–916.
6. Ilieva EV, Ayala V, Jové M, Dalfó E, Cacabelos D, Povedano M, Bellmunt MJ, Ferrer I, Pamplona R, Portero-Otín M (2007) Oxidative and endoplasmic reticulum stress interplay in sporadic amyotrophic lateral sclerosis. *Brain* **130**: 3111–3123.
7. Cacabelos D, Ayala V, Ramírez-Nunez O, Granado-Serrano AB, Boada J, Serrano JCE, Cabré R, Nadal-Rey G, Bellmunt MJ, Ferrer I, et al. (2014) Dietary lipid unsaturation influences survival and oxidative modifications of an amyotrophic lateral sclerosis model in a gender-specific manner. *Neuromolecul Med* **16**: 669–685.
8. Du Z-W, Chen H, Liu H, Lu J, Qian K, Huang C-L, Zhong X, Fan F, Zhang S-C (2015) Generation and expansion of highly pure motor neuron progenitors from human pluripotent stem cells. *Nat Commun* **6**: 6626.
9. Blobel G, Potter VR (1966) Nuclei from rat liver: isolation method that combines purity with high yield. *Science* **154**: 1662–1665.
10. Jové M, Moreno-Navarrete JM, Pamplona R, Ricart W, Portero-Otín M, Fernández-Real JM (2014) Human omental and subcutaneous adipose tissue exhibit specific lipidomic signatures. *FASEB J* **28**: 1071–1081.
11. Grimm MOW, Kuchenbecker J, Rothhaar TL, Grösgen S, Hundsdörfer B, Burg VK, Friess P, Müller U, Grimm HS, Riemenschneider M, et al. (2011) Plasmalogen synthesis is regulated via alkyl-

dihydroxyacetonephosphate-synthase by amyloid precursor protein processing and is affected in Alzheimer's disease. *J Neurochem* **116**: 916–925.

12. Starodub O, Jolly CA, Atshaves BP, Roths JB, Murphy EJ, Kier AB, Schroeder F (2000) Sterol carrier protein-2 localization in endoplasmic reticulum and role in phospholipid formation. *Am J Physiol Cell Physiol* **279**: C1259–69.
13. Benador IY, Veliova M, Mahdaviani K, Petcherski A, Wikstrom JD, Assali EA, Acín-Pérez R, Shum M, Oliveira MF, Cinti S, et al. (2018) Mitochondria Bound to Lipid Droplets Have Unique Bioenergetics, Composition, and Dynamics that Support Lipid Droplet Expansion. *Cell Metab* **27**: 869–885.e6.
14. Nishimura AL, Mitne-Neto M, Silva HCA, Richieri-Costa A, Middleton S, Cascio D, Kok F, Oliveira JRM, Gillingwater T, Webb J, et al. (2004) A mutation in the vesicle-trafficking protein VAPB causes late-onset spinal muscular atrophy and amyotrophic lateral sclerosis. *Am J Hum Genet* **75**: 822–831.
15. Boeynaems S, Bogaert E, Van Damme P, Van Den Bosch L (2016) Inside out: the role of nucleocytoplasmic transport in ALS and FTLD. *Acta Neuropathol* **132**: 159–173.
16. Mészáros N, Cibulka J, Mendiburo MJ, Romanauska A, Schneider M, Köhler A (2015) Nuclear pore basket proteins are tethered to the nuclear envelope and can regulate membrane curvature. *Dev Cell* **33**: 285–298.
17. Floch AG, Tareste D, Fuchs PFJ, Chadrin A, Naciri I, Léger T, Schlenstedt G, Palancade B, Doye V (2015) Nuclear pore targeting of the yeast Pom33 nucleoporin depends on karyopherin and lipid binding. *J Cell Sci* **128**: 305–316.
18. Stavru F, Nautrup-Pedersen G, Cordes VC, Görlich D (2006) Nuclear pore complex assembly and maintenance in POM121- and gp210-deficient cells. *J Cell Biol* **173**: 477–483.
19. Doucet CM, Hetzer MW (2010) Nuclear pore biogenesis into an intact nuclear envelope. *Chromosoma* **119**: 469–477.
20. Patel SS, Rexach MF (2008) Discovering novel interactions at the nuclear pore complex using bead halo: a rapid method for detecting molecular interactions of high and low affinity at equilibrium. *Mol Cell Proteomics* **7**: 121–131.
21. Irvine RF (2003) Nuclear lipid signalling. *Nat Rev Mol Cell Biol* **4**: 349–360.
22. Montaña M, García del Caño G, López de Jesús M, González-Burguera I, Echeazarra L, Barrondo S, Sallés J (2012) Cellular neurochemical characterization and subcellular localization of phospholipase C β1 in rat brain. *Neuroscience* **222**: 239–268.
23. Yasuda E, Nagasawa K, Nishida K, Fujimoto S (2008) Decreased expression of phospholipase C-beta 1 protein in endoplasmic reticulum stress-loaded neurons. *Biol Pharm Bull* **31**: 719–721.
24. Dalfó E, Albasanz JL, Rodríguez A, Martín M, Ferrer I (2005) Abnormal group I metabotropic glutamate receptor expression and signaling in the frontal cortex in Pick disease. *J Neuropathol Exp Neurol* **64**: 638–647.
25. Rodríguez A, Freixes M, Dalfó E, Martín M, Puig B, Ferrer I (2005) Metabotropic glutamate receptor/phospholipase C pathway: a vulnerable target to Creutzfeldt-Jakob disease in the cerebral cortex. *Neuroscience* **131**: 825–832.
26. Böhm D, Schwegler H, Kotthaus L, Nayernia K, Rickmann M, Köhler M, Rosenbusch J, Engel W, Flügge G, Burfeind P (2002) Disruption of PLC-beta 1-mediated signal transduction in mutant mice causes age-dependent hippocampal mossy fiber sprouting and neurodegeneration. *Mol Cell Neurosci* **21**: 584–601.
27. Kim D, Jun KS, Lee SB, Kang NG, Min DS, Kim YH, Ryu SH, Suh PG, Shin HS (1997) Phospholipase C isozymes selectively couple to specific neurotransmitter receptors. *Nature* **389**: 290–293.
28. Battaglia G, Bruno V (2018) Metabotropic glutamate receptor involvement in the pathophysiology of amyotrophic lateral sclerosis: new potential drug targets for therapeutic applications. *Curr Opin Pharmacol* **38**: 65–71.
29. Hu JH, Zhang H, Wagey R, Krieger C, Pelech SL (2003) Protein kinase and protein phosphatase expression in amyotrophic lateral sclerosis spinal cord. *J Neurochem* **85**: 432–442.
30. Krupska O, Sarnowska A, Fedorczyk B, Gewartowska M, Misicka A, Zablocka B, Beresewicz M (2017) Ischemia/Reperfusion-Induced Translocation of PKCβII to Mitochondria as an Important Mediator of a Protective Signaling Mechanism in an Ischemia-Resistant Region of the Hippocampus. *Neurochem Res* **42**: 2392–2403.
31. Patergnani S, Marchi S, Rimessi A, Bonora M, Giorgi C, Mehta KD, Pinton P (2013) PRKCB/protein kinase C, beta and the mitochondrial axis as key regulators of autophagy. *Autophagy* **9**: 1367–1385.
32. Torres P, Ramírez-Núñez O, Romero-Guevara R, Barés G, Granado-Serrano AB, Ayala V, Boada J, Fontdevila L, Povedano M, Sanchís D, et al. (2018) Cryptic exon splicing function of TARDBP interacts with autophagy in nervous tissue. *Autophagy* **14**: 1398–1403.
33. Vandoorne T, De Bock K, Van Den Bosch L (2018) Energy metabolism in ALS: an underappreciated opportunity? *Acta Neuropathol* **135**: 489–509.

34. Lessig J, Fuchs B (2009) Plasmalogens in biological systems: their role in oxidative processes in biological membranes, their contribution to pathological processes and aging and plasmalogen analysis. *Curr Med Chem* **16**: 2021–2041.
35. Albert CJ, Anbukumar DS, Monda JK, Eckelkamp JT, Ford DA (2007) Myocardial lipidomics. Developments in myocardial nuclear lipidomics. *Front Biosci* **12**: 2750–2760.
36. Cacabelos D, Ayala V, Granado-Serrano AB, Jové M, Torres P, Boada J, Cabré R, Ramírez-Núñez O, Gonzalo H, Soler-Cantero A, et al. (2016) Interplay between TDP-43 and docosahexaenoic acid-related processes in amyotrophic lateral sclerosis. *Neurobiol Dis* **88**: 148–160.
37. Farese RV, Walther TC (2016) Lipid droplets go nuclear. *J Cell Biol* **212**: 7–8.
38. Romanauska A, Köhler A (2018) The Inner Nuclear Membrane Is a Metabolically Active Territory that Generates Nuclear Lipid Droplets. *Cell* **174**: 700–715.e18.
39. Ioannou MS, Jackson J, Sheu S-H, Chang C-L, Weigel AV, Liu H, Pasolli HA, Xu CS, Pang S, Matthies D, et al. (2019) Neuron-Astrocyte Metabolic Coupling Protects against Activity-Induced Fatty Acid Toxicity. *Cell*.
40. Liu L, Zhang K, Sandoval H, Yamamoto S, Jaiswal M, Sanz E, Li Z, Hui J, Graham BH, Quintana A, et al. (2015) Glial lipid droplets and ROS induced by mitochondrial defects promote neurodegeneration. *Cell* **160**: 177–190.
41. Dodge JC, Treleaven CM, Pacheco J, Cooper S, Bao C, Abraham M, Cromwell M, Sardi SP, Chuang W-L, Sidman RL, et al. (2015) Glycosphingolipids are modulators of disease pathogenesis in amyotrophic lateral sclerosis. *Proc Natl Acad Sci USA* **112**: 8100–8105.
42. Henriques A, Croixmarie V, Priestman DA, Rosenbohm A, Dirrig-Grosch S, D'Ambra E, Huebecker M, Hussain G, Boursier-Neyret C, Echaniz-Laguna A, et al. (2015) Amyotrophic lateral sclerosis and denervation alter sphingolipids and up-regulate glucosylceramide synthase. *Hum Mol Genet* **24**: 7390–7405.
43. Guenther GG, Edinger AL (2009) A new take on ceramide: starving cells by cutting off the nutrient supply. *Cell Cycle* **8**: 1122–1126.
44. Cascianelli G, Villani M, Tosti M, Marini F, Bartoccini E, Magni MV, Albi E (2008) Lipid microdomains in cell nucleus. *Mol Biol Cell* **19**: 5289–5295.

FIGURE LEGENDS

Fig. 1 Whole nuclei could be enriched from frozen spinal cords. a) Schematic procedure for obtention of a nuclei enriched fraction departing from frozen human spinal cords. b) Immunocytochemical evidence for nuclei integrity and heterogeneity, as shown by immunolabeling of nucleoporin (Mab414), by presence of neuron specific tubulin ß III (TubIII) and DAPI possitivity (in blue). c) Nuclei enriched fraction is depleted from cytosolic and other membrane containing organelle (such as mitochondria), as indicated by lack of immunoreactivity for mitochondrial markers (porin and mitofusin) and selective improvement in nuclear antigens (poly-ADP-ribose polimerase (PARP) and histone-H3)

Fig. 2 Nuclei from ALS patients exhibit a specific lipidome. Multivariate analyses including PCA (a), partial least square-discriminant analyses (b) and hierarchical clustering analyses (c, using lipids significantly affected by ALS status) demonstrate that nuclei from ALS patients exhibit a specific lipidomic profile. Upper panels are

obtained by using lipids ionized in positive ionization, while as lower panels show the results using negative ionization

Fig. 3 Changes in nuclear DAG concentrations suggested by lipidomics are associated with alterations in PLCßI and PKCßII levels in ALS. Representative western-blot analyses of PKCßII in spinal cord lysates from ALS patients (a) and G93A mice (at terminal stage, 150 days, b) show that protein concentration is decreased in comparison with adequate control. Similarly, western-blot analyses of PLCßI are also decreased in spinal cord lysates from ALS patients (c) and G93A mice (d). In all panels, upper part shows representative western-blot images with lower part demonstrating quantification by densitometry, after normalization by Coomassie blue staining. Differences between groups were analyzed by Student's t test.

Fig. 4 Changes in nuclear plasmalogen concentrations suggested by lipidomics are associated with alterations in AGPS in human motor neurons and in G93A mice. Representative western-blot analyses of AGPS in spinal cord lysates from G93A mice (at terminal stage, 150 days, a) and ALS patients (b) show that protein concentration is decreased in G93A mice in comparison with adequate controls. c) confocal imaging of hIPs-derived motor neurons demonstrates decreased levels in cells derived from *FUS* mutants and C9orf72 IPs, as shown by quantiatiative analyses (see right panel in c); further, there was a significant correlation between AGPS cell content and nuclear perimeter (see below panels from each picture) both in control and in C9orf72 cells, but this was lost in *FUS* mutated cells. d) shows that confocal immunohistochemistry analyses of ventral regions of lumbar spinal cord section demonstrate a strong reactivity of AGPS in motor neurons in non-transgenic mice (arrows) in comparison with G93A mice (arrowheads). Motor neurons were identified by size, nuclear morphology and tubulin ßIII immunoreactivity. Right panel in d shows quantitative analyses of AGPS immunoreactivity in these cells, compatible with decreased expression of this protein. In a) and b) panels, upper part shows representative western-blot images with lower part demonstrating quantification by densitometry, after normalization by Coomassie blue staining. Differences between groups were analyzed by Student's t test (a and d) and by ANOVA followed by Bonferroni post-hoc analyses in c. Bars in c and d are 10 µM long.

Fig. 5 Changes in nuclear phospholipid and ether-phospholipids concentrations suggested by lipidomics are associated with alterations in SCP-2 in G93A mice. a) Confocal immunohistochemistry analyses of PMP70 in ventral regions of lumbar spinal cord sections, with an enrichment in PMP70 in motor neurons in G93A mice (at terminal stage, 150 days, arrows) in comparison with non-transgenic mice. Motor neurons were identified by size and nuclear morphology. b) As evidenced by western-blot analyses of PMP70 in spinal cord lysates, G93A mice do not show a general increase in PMP70 (quantification in e, after normalization by Coomassie blue staining). In line with potential ER/peroxisomal changes, immunoreactivity of SCP-2 is severely affected by G93A overexpression (c). While in non-Tg specimens, SCP-2 formed a perinuclear rim, this pattern is lost in G93A with enhancement in vesicular structures, specifically found in motor neurons. This is accompanied by an increase in the total lysate concentration of SCP-2, as shown by western blot analyses (in d and e). Differences between non-Tg and G93A were analyzed by Student's t test. Bars in A and C are 10 μM long.

Fig. 6 Isolated nuclei show structures compatible with lipid droplets. Confocal image of isolated nuclei, showing Nile Red fluorescent vesicles both in the periphery of the nuclei (upper panel) or even inside the nuclear matrix (lower panel). Bars are 10 μM long.

TABLES

Table 1

Characteristics of tissue donors.

Gender	Age at death	Diagnosis	Disease onset	Disease duration	Postmortem delay
M	64	ALS	Bulbar	2 years	16h 30 m
M	57	ALS	Bulbar	2 years	4h
F	75	ALS	Bulbar	4 years	4h 5m
F	79	ALS	Bulbar	20 months	2h 10m

M	74	-	-	-	10h 50m
F	78	-	-	-	5h
M	66	-	-	-	4h 20m
M	86	-	-	-	18h 15m

Table 2

Media used for human motor neuron differentiation from iPSC.

Component\Media	**NEPM**	**MNP media 1st**	**MNP med 2nd**	**MN induction med**	**MN maturation media**
DM/F12	20 ml	20 ml			
Neurobasal	20 ml	20 ml			
Neurobasal +			40 ml	40 ml	40 ml
B27+ supplement	800 µl	800 µl	800 µl	800 µl	800 µl
Ascorbic acid	0.1 mM	0.1 mM	0.1 mM	0.1 mM	0.1 mM
L-Glutamine solution (Thermo Scientific, # 25030024)	1:200	1:200	1:200	1:200	1:200
Non essential amino acid solution (Sigma, M7145)	1:100	1:100	1:100	-	-
CHIR	3 µM	1 µM	3 µM	3 µM	
SB43	2 µM	2 µM	2 µM	2 µM	
DMH1	2 µM	2 µM	2 µM	2 µM	
Retinoic acid		0.1 µM	0.1 µM	0.5 µM	0.5 µM
Purmorphamine		0.5 µM	0.5 µM	0.1 µM	0.1 µM
Valproic acid			0.5 mM		
Compound E					0.1 µM

CNTF					20 ng/ml
IGF1					20 ng/ml
Penicillin/Streptromycin (Thermo Scientific # 15140122)	1:400	1:400	1:400	1:400	1:400

Table 3

Antibodies and conditions used.

Target	Dilution	Reference
PARP	1:500 in TBS-T 0.05%[1]	sc-74470 (Santa Cruz Biotechnology)
Histone H3	1:500 in TBS-T 0.05%	SAB4500352 (Sigma-Aldrich)
Mitofusin 2	1:1000 in TBS-T 0.05%	M6319 (Sigma-Aldrich)
Porin	1:1000 in TBS-T 0.05%	ab15895 (Abcam)
Lactate dehydrogenase	1:1000 in TBS-T 0.05%	ab135396 (Abcam)
Nuclear Pore Complex Proteins [Mab414]	1:250 in PBS	ab50008 (Abcam)
Tubulin βIII	1:250 in PBS	ab18207 (Abcam)
AGPS	1:250 in TBS-T 0.05% for western blot; 1:150 in PBS for immunofluorescence	sc-374201 (Santa Cruz Biotechnology)
PLC βI	1:250 in TBS-T 0.05%	sc-5291 (Santa Cruz Biotechnology)
PKC βII	1:250 in TBS-T 0.05%	sc-13149 (Santa Cruz Biotechnology)
SCP-2	1:1000 in TBS-T 0.05%	hpa027135 (Atlas Antibodies)
PMP70	1:250 in PBS	Ab3421 (Abcam)
Mouse IgG, Alexa Fluor® 488 conjugate	1:800 in PBS	A-11001 (Thermo Fisher Scientific)

Rabbit IgG, Alexa Fluor® 546 conjugate	1:800 in PBS	A-11010 (Thermo Fisher Scientific)
Rabbit IgG, horseradish peroxidase conjugate	1:50000 in TBS-T 0.05%	31460 (Thermo Fisher Scientific)
Rabbit IgG, horseradish peroxidase conjugate	1:30000 in TBS-T 0.05%	NA931V (Sigma)

[1] TBS-T 0.05%: Tris Buffered Saline with Tween-20 0.05%

Table 4

Differential lipids in nuclei isolated from ALS patients in comparison to non-ALS

Potential ID[1]	P value[2]	Change(ALS vs non-ALS)
Diacylglycerols		
DG(34:2)[3][iso2]	0,017499	down
DG(46:3)/CE(24:0)	0,027414	down
DG(36:0) [3]	0,023379	down
DG(36:2) [3]	0,010411	down
DG(39:7)[[3]/PA(O-32:0)	0,007198	up
DG(35:1) [3]	0,025619	up
DG(36:0) [3]	0,001003	up
DG(38:0) [3]	0,002498	up
DG(39:6) [3]	0,034444	up
Glycerophospholipids		
PA(18:0)	0,024149	down
PA(O-36:3))/PG(O-29:0)	0,043124	down

PG(P-40:2)/PG(O-40:3)	0,027358	down
PS(O-40:1)/PS(P-40:0)/ PS(39:1)/	0,015925	down
PE(P-42:1)/ PE(O:42:2)/PE(42:1)/GlcCer(d36:0)/PC(39:1)	0,029046	down
PA(O-32:0)	0,024342	up
PA(P-37:0)/PG(32:0)/PA(38:5)	0,018452	up
PA(P-35:1)	0,018294	up
PC(O-24:0)	0,0235	up
PE(42:10)/PI(31:1)	5,35E-05	up
PE(O-37:1)/)/ PC(P-33:2)/PE(P-36:2)/PE(O-36:3)/Cerebroside B/ GlcCer(35:2)/CerP(42:2)	0,024172	up
PE(P-38:3)/PE(38:3)/PC(O-35:4)/PE-NMe2(36:2)/PE(O-38:4	4,76E-04	up
PG(33:2)	0,025597	up
PG(O-38:1)/PG(P-38:0)/PG(38:0)/TG(48/8)	0,025968	up
PG(P-37:1)/PG(O-37:2)	0,022001	up
PS(P-38:4)/PS(O-38:5)/PI(O-32:0)/PC(37:4)/PE(40:4)	0,01172	up
PS(P-38:4)/PS(O-38:5)	0,025977	up
PE(P-38:3)/PE(38:3)/PC(O-35:4)/ PE(O-38:4)/Cerebroside C/	0,011598	up
Triacylglycerols		
TG(46:1)	0,029092	down
TG(48:2)	0,028442	down
TG(50:3)/PG(41:0)	0,027652	down
TG(60:7)	0,019288	down
TG(43:3)/PE-Cer(39:1)/SM(36:1)/PA(P-39:0)/PA(O-39:1)	0,027467	down
TG(54:3)	0,01669	up
TG(65:12)	0,001038	up
TG(50:0)	0,027069	up
TG(59:9)	0,00401	up
TG(65:2)	0,001892	up
Sphingolipids		

Cer(d35:0)	0,027563	down
GlcCer(d42:1)/PC(38:1)/PE(41:1)	0,026204	down
Cer(46:0)	0,007346	up
LacCer(d34:0)/PC(42:5)/Ins-1-P-Cer(40:1)/C22 Sulfatide	0,025398	up

[1] LIPID-MAPS nomenclature, identification has been proposed on basis of isotope distribution and identity of retention times with those of representative standards, except in [3] where identity was confirmed by MS/MS; [2] p value after T test for differences

Figure 1

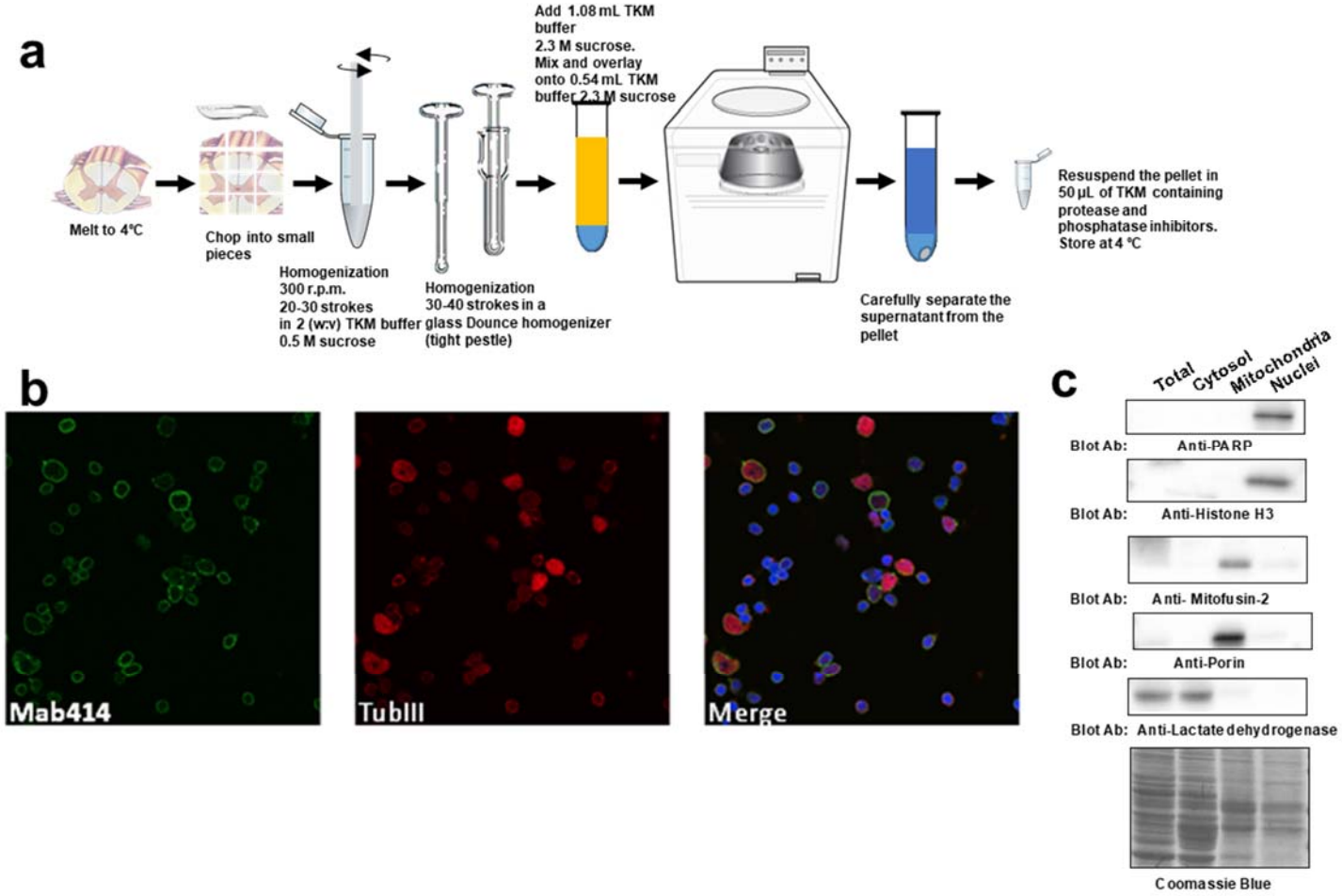

Figure 2

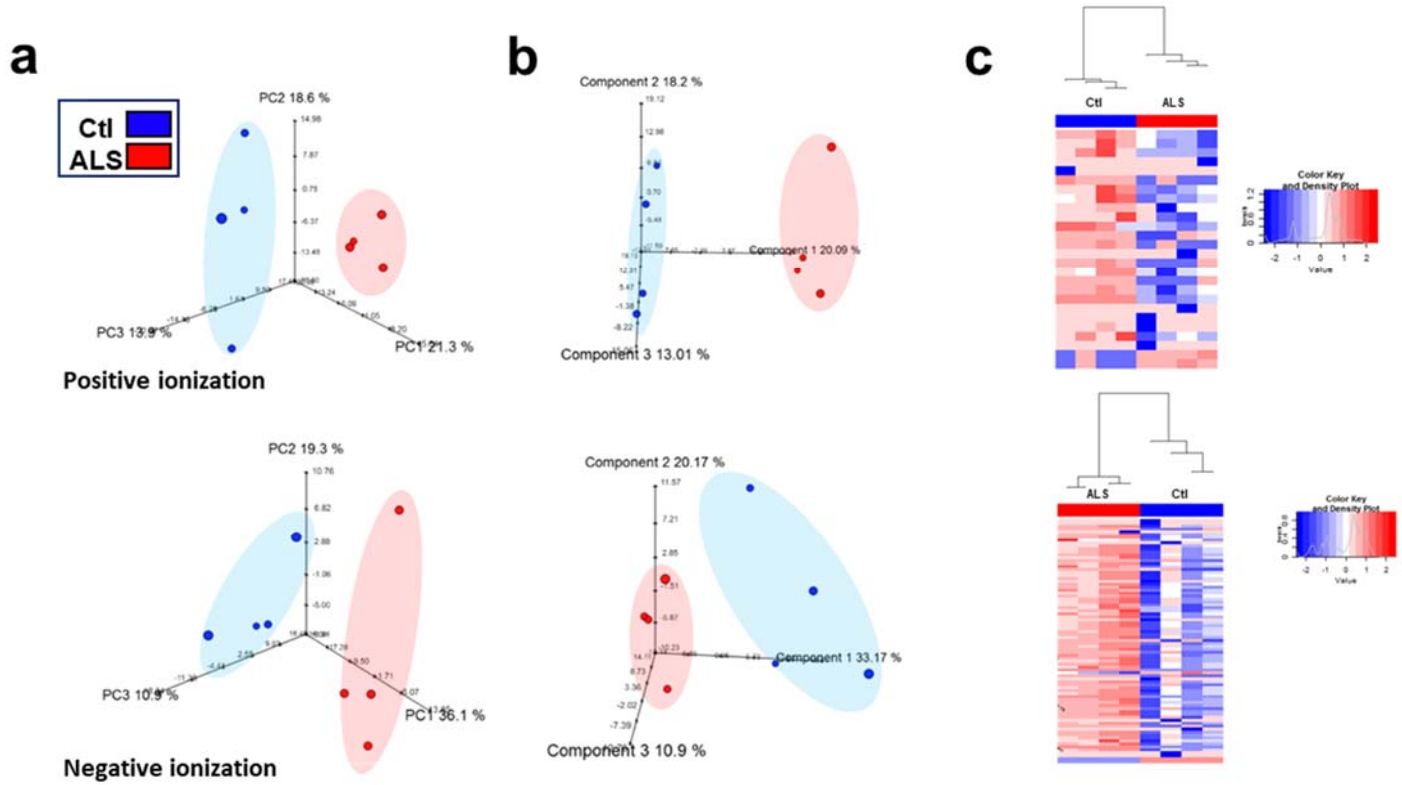

Figure 3

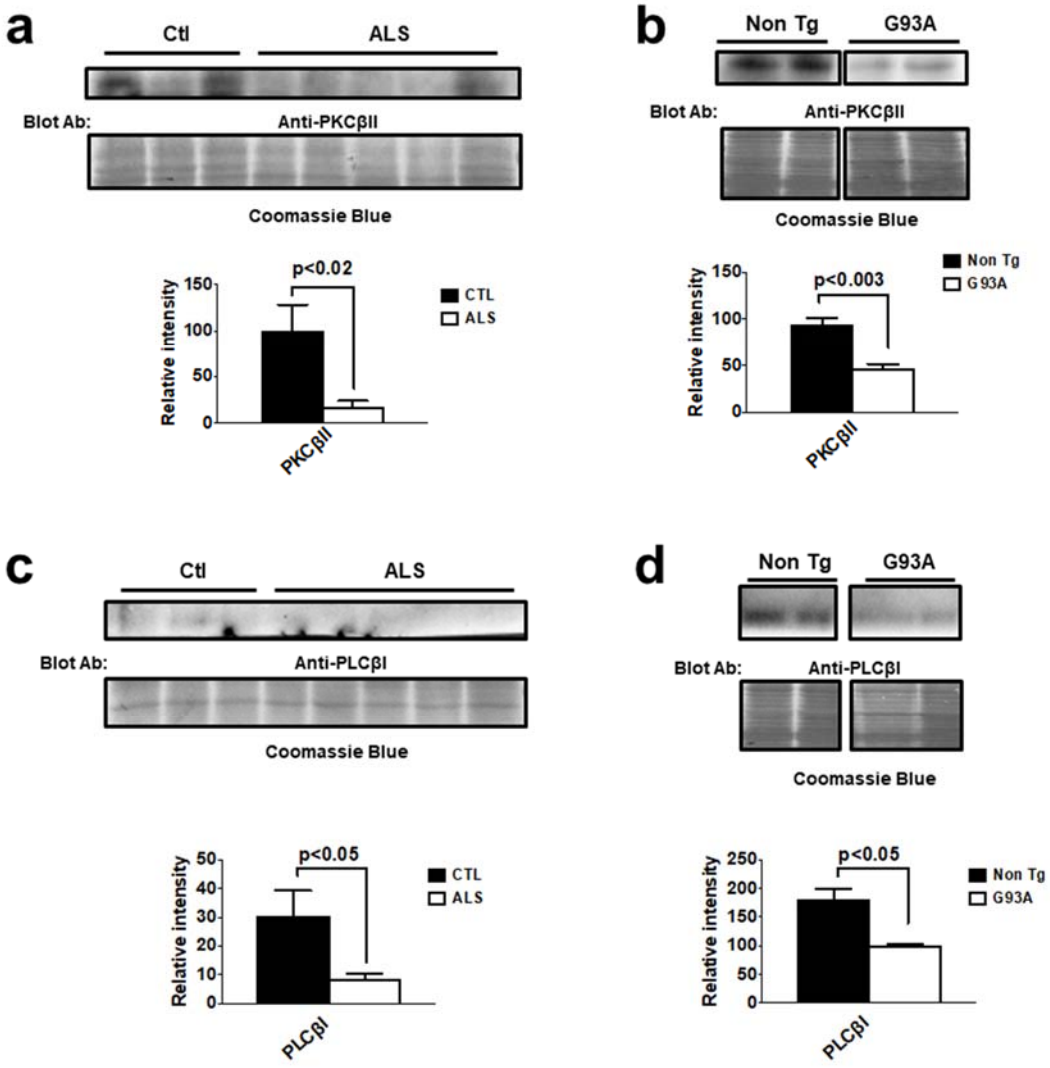

Figure 4

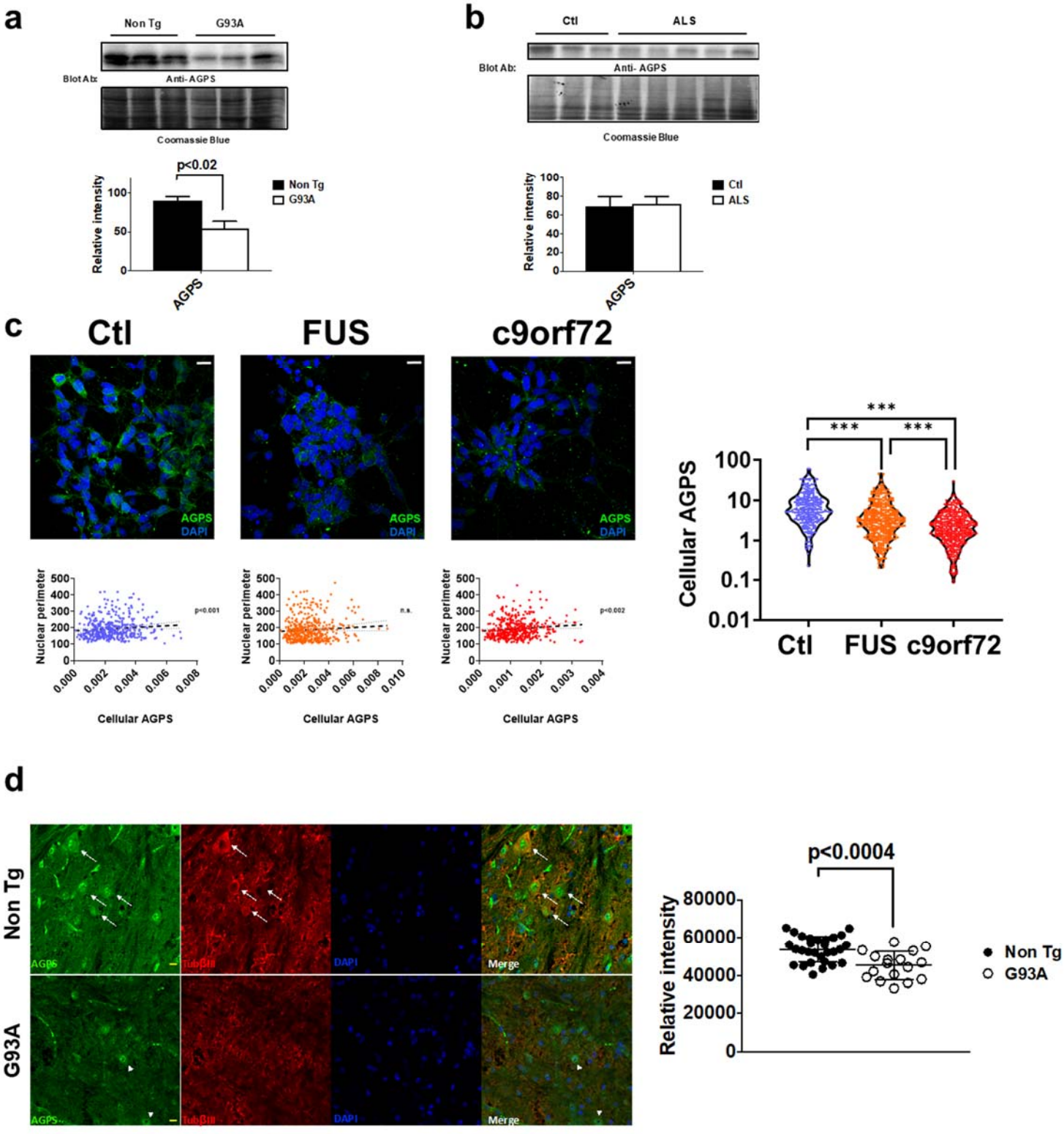

Figure 5

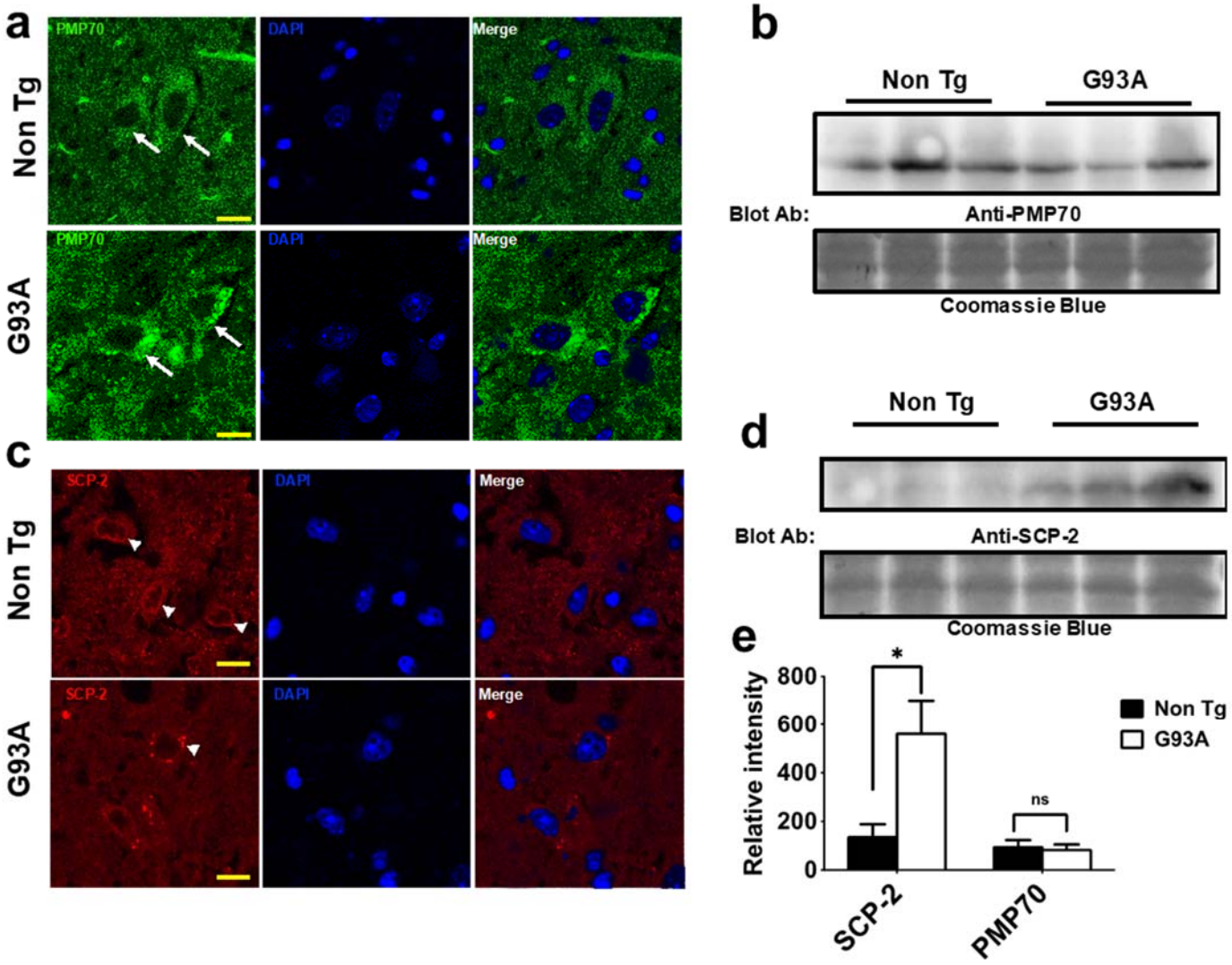

Figure 6

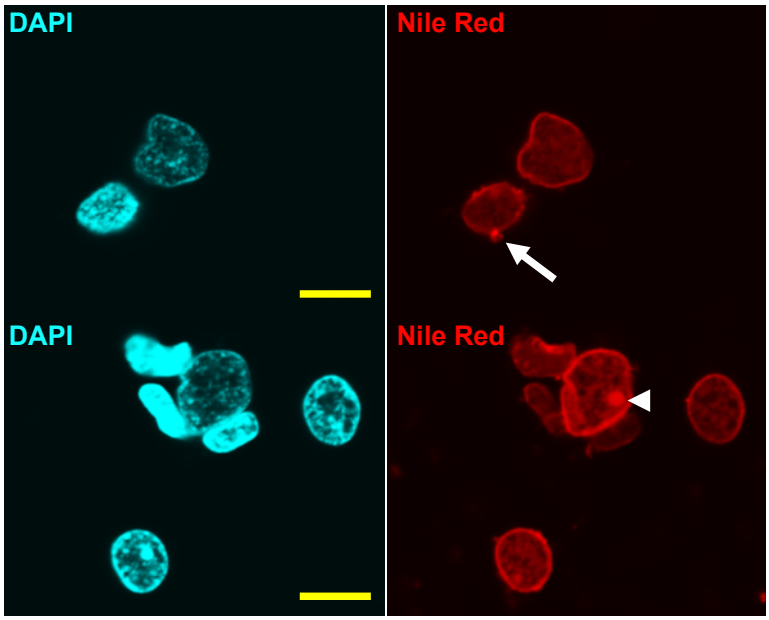

Compound
392.2951@10.1815
719.6055@9.690249
PE42:10) / PS(38:4) / PI(31:1)
935.5716@10.32
823.4462@9.345625
591.5298@9.67875
537.5588@9.947374
PE-NMe2(36:2) / Cerebroside C / PE(P-38:3) / PC(O-35:4) / PE(O-38:4)
509.528@9.689125
795.4147@9.01925
613.7038@7.652
879.5086@9.887375
DG(36:0)
781.4012@9.0195
566.6927@7.651
851.4783@9.62225
240.2442@10.41038
495.5118@9.529125
567.6986@7.6485
242.2597@10.41013
798.3992@9.020625
809.4308@9.34525
567.4859@9.679249
907.5388@10.11962
647.5615@9.68425
633.5588@8.513376
481.4959@9.373624
942.7914@10.43637
645.4982@9.685876
TG(59:9)
767.3841@8.648625
634.5134@7.888876
882.4914@9.886624
Cer(d46:0)
242.2601@7.887875
725.3374@8.226375
572.5035@7.988875
739.353@8.226999
506.5045@7.88725
753.3713@8.647875
508.5217@7.88775
605.5148@9.677375
673.5342@9.6826
643.4132@9.6798
896.7988@5.293799
689.6095@9.6846

836.7786@10.0204
697.3067@7.739801
808.7509@10.409
711.3218@7.7455
478.5098@10.40963
654.543@8.578875
1062.8143@10.766999
1025.0608@9.682
1019.0572@9.681625
TG(65:12)
883.8483@9.727125
C35 H68 O4 - 6.345625
C35 H69 N O7
941.6179@6.7009997
PA(P-35:1)
C35 H68 O4
548.0226@9.683
LacCer(d34:0)
C20 H38 Cl N9 O10 S
PG(33:2)
608.515@9.676999
C33 H69 N3 O

PA(O-36:3)
Cerebroside C / PE(P-38:3) / PC(O-35:4) / PE(O-38:4)
PI(O-32:0) / PE(40:4) / PC(37:4)
PS(39:1) / PS(O-40:1) / PS(P-40:0)
DG(34:2)
TG(60:7)
856.8291@10.62438
C17 H40 N6 O2
PA(P-37:0)
C15 H27 N5
DG(32:0)
PE(48:0)
C21 H45 N5
PE(O-37:1)
903.8038@10.643
Glucosylceramide (d42:1)
CE(24:0)

Cer(d35:0)
TG(50:3)
TG(48:2)
GlcCer(d42:0)
TG(46:1)

Log FC	p	FC (abs)	Regulation	FC	Abund Diff (Raw)
-18.29531	9.46787E-15	321689.03	down	-321689	-296709.34
14.330662	2.70109E-11	20604.355	up	20604.355	22338.002
0.3022712	5.35038E-05	1.2330841	up	1.2330841	12307.934
0.4281497	0.000179481	1.3455068	up	1.3455068	8780.457
0.3373814	0.000313269	1.2634612	up	1.2634612	66141.05
0.2663202	0.000353472	1.2027361	up	1.2027361	37949.78
0.2918873	0.00045163	1.2242408	up	1.2242408	81996.31
0.2676515	0.000476271	1.2038466	up	1.2038466	244366.44
0.1971655	0.000528097	1.1464437	up	1.1464437	9519584
0.247962	0.000738498	1.1875284	up	1.1875284	46105.22
0.3843689	0.000789941	1.3052887	up	1.3052887	77908.05
0.2968307	0.000944302	1.2284428	up	1.2284428	30871.133
0.2659974	0.001002614	1.2024671	up	1.2024671	81224.625
0.2742546	0.001153632	1.2093691	up	1.2093691	10125.514
0.1899328	0.001224027	1.1407106	up	1.1407106	78520.69
0.2368284	0.001269561	1.1783992	up	1.1783992	38554.297
0.4355783	0.001425651	1.3524529	up	1.3524529	19754.68
0.2540265	0.001465978	1.1925308	up	1.1925308	46568.484
0.1754923	0.001635774	1.1293497	up	1.1293497	199240
0.2594014	0.001716011	1.1969819	up	1.1969819	52603.938
0.2435737	0.001727314	1.1839217	up	1.1839217	4261.241
0.2414604	0.001904014	1.1821887	up	1.1821887	12430.402
0.2039666	0.00234749	1.151861	up	1.151861	46603.812
0.2285686	0.002423955	1.1716719	up	1.1716719	14305.125
0.5558435	0.002497559	1.4700279	up	1.4700279	43906.15
0.2173128	0.003505627	1.1625662	up	1.1625662	357430.25
0.2932372	0.003669221	1.2253867	up	1.2253867	29396.71
0.5801316	0.004009763	1.4949856	up	1.4949856	8723.716
0.6990976	0.004385273	1.623489	up	1.623489	16319.041
0.4774783	0.005379546	1.3923079	up	1.3923079	6620.994
0.1634058	0.005539431	1.1199279	up	1.1199279	32828.64
0.3394746	0.007197958	1.2652957	up	1.2652957	15155.879
0.1752267	0.007275474	1.1291418	up	1.1291418	3385.4326
0.3580788	0.007345918	1.2817179	up	1.2817179	7310.084
0.1522627	0.007694131	1.1113111	up	1.1113111	40808.656
0.29724	0.007980905	1.2287914	up	1.2287914	5920.3984
0.3211696	0.008076015	1.249343	up	1.249343	8913.504
0.1192103	0.010608972	1.0861402	up	1.0861402	23971.531
0.1899233	0.013492855	1.1407031	up	1.1407031	4630.6406
0.2688942	0.01398979	1.2048839	up	1.2048839	7713.291
0.1186428	0.014853423	1.085713	up	1.085713	186070.75
0.19807	0.016001929	1.1471627	up	1.1471627	30542.516
10.458794	0.019507704	1407.3774	up	1407.3774	15544.826
10.053368	0.020231474	1062.5887	up	1062.5887	10946.303
10.482759	0.020504646	1430.9519	up	1430.9519	16313.437
10.459054	0.021393746	1407.6315	up	1407.6315	16400.215

9.88291	0.02147479	944.17456	up	944.17456	9688.325
10.239968	0.021548705	1209.3099	up	1209.3099	13472.254
9.693098	0.021708582	827.77686	up	827.77686	7917.038
0.1072568	0.024238328	1.0771781	up	1.0771781	14087.383
0.1969139	0.027149547	1.1462438	up	1.1462438	5494.1953
0.3274932	0.03444416	1.2548311	up	1.2548311	10787.836
-14.23055	9.58254E-13	19223.04	down	-19223.04	-17729.363
14.412014	8.52619E-12	21799.6	up	21799.6	23633.838
13.484619	2.18989E-11	11462.381	up	11462.381	12426.362
0.2754636	0.00052883	1.2103829	up	1.2103829	2358656
0.3807897	0.001037565	1.3020544	up	1.3020544	35438.984
0.1650462	0.001308356	1.121202	up	1.121202	44652.766
0.432534	0.001892372	1.349602	up	1.349602	37389.67
0.5440353	0.002141869	1.458045	up	1.458045	8311.903
0.2251273	0.006784787	1.1688803	up	1.1688803	24337.11
0.3945727	0.008297467	1.3145534	up	1.3145534	13978.539
0.2971216	0.008873323	1.2286905	up	1.2286905	115504.72
-0.215548	0.010410988	1.1611445	down	-1.161145	-5677.633
-0.280678	0.012372271	1.2147657	down	-1.214766	-1966.8125
0.2645808	0.016690265	1.2012869	up	1.2012869	8771.291
0.6036241	0.018294131	1.5195289	up	1.5195289	9538.023
0.1995873	0.019939106	1.1483698	up	1.1483698	10893.824
0.273346	0.020230094	1.2086077	up	1.2086077	5842.6504
-11.40286	0.021313224	2707.7231	down	-2707.723	-2496.4673
-11.52748	0.022939231	2951.9966	down	-2951.997	-37045.53
-13.02247	0.023617232	8320.608	down	-8320.608	-150396.84
-0.208895	0.02364707	1.1558024	down	-1.155802	-4493.742
-11.13556	0.02414891	2249.7627	down	-2249.763	-2074.0693
11.258992	0.024290718	2450.7239	up	2450.7239	2656.0442
9.943075	0.02434156	984.3825	up	984.3825	1066.2552
10.488378	0.024457032	1436.5352	up	1436.5352	1556.4735
11.066494	0.024697773	2144.6016	up	2144.6016	2324.1504
11.624372	0.02506041	3157.0723	up	3157.0723	3421.8584
11.315565	0.025080454	2548.7341	up	2548.7341	2762.304
9.327595	0.025298784	642.51874	up	642.51874	695.61035
10.794524	0.025398463	1776.1333	up	1776.1333	1924.6616
10.314449	0.025425991	1273.3818	up	1273.3818	1379.5837
10.506367	0.025469834	1454.5597	up	1454.5597	1576.0144
9.624341	0.025549063	789.25134	up	789.25134	854.6965
11.656177	0.025596691	3227.4446	up	3227.4446	3498.1528
9.55644	0.02561899	752.9657	up	752.9657	815.3555
11.000752	0.025693204	2049.0684	up	2049.0684	2220.573
0.2186685	0.025736462	1.1636591	up	1.1636591	8916.699
11.316339	0.025968196	2550.1008	up	2550.1008	2763.7856
11.896506	0.025977213	3812.4595	up	3812.4595	4132.4185
0.340884	0.027068563	1.2665324	up	1.2665324	4817.218
0.2631978	0.032180473	1.200136	up	1.200136	6826.1465

0.1703036	0.034483775	1.1252953	up	1.1252953	5812.5195
-0.070622	0.039186444	1.0501693	down	-1.050169	567.87695
0.2115406	0.03973117	1.157924	up	1.157924	4067.289
-0.685736	0.04312377	1.6085223	down	-1.608522	-28952.445
0.4922731	0.04570038	1.4066595	up	1.4066595	12174.039
0.4334636	0.049116958	1.3504719	up	1.3504719	51009.453
11.690846	0.011598373	3305.9436	up	3305.9436	28635.693
11.976217	0.011720145	4029.0312	up	4029.0312	37497.65
-10.65984	0.015925	1617.8226	down	-1617.823	-17041.242
-12.55013	0.016834518	5997.439	down	-5997.439	-98068.49
-10.85686	0.017498925	1854.5525	down	-1854.553	-20897.605
-9.989641	0.019287597	1016.6738	down	-1016.674	-10038.737
-0.445942	0.035632934	1.3622036	down	-1.362204	-759257
12.730565	0.016436499	6796.4473	up	6796.4473	82760.18
10.624329	0.018451843	1578.4891	up	1578.4891	14042.712
10.180083	0.021526989	1160.14	up	1160.14	1024.5553
10.648276	0.021528255	1604.9097	up	1604.9097	1417.7284
10.731791	0.021985058	1700.5557	up	1700.5557	1502.2788
10.806344	0.022001365	1790.7448	up	1790.7448	1582.0054
11.637106	0.023172377	3185.0625	up	3185.0625	2814.572
-10.07715	0.023353804	1080.2491	down	-1080.249	-1221.0115
-11.43544	0.023378903	2769.5654	down	-2769.565	-3132.0183
-11.1456	0.023444695	2265.4744	down	-2265.474	-2561.775
-9.776294	0.023451306	876.91534	down	-876.9153	-990.9939
11.925119	0.023500301	3888.8271	up	3888.8271	3436.6948
-10.8379	0.023510749	1830.3417	down	-1830.342	-2069.5393
13.176004	0.02374818	9254.917	up	9254.917	8180.2847
-13.03395	0.023875253	8387.067	down	-8387.067	-194685.02
11.992132	0.024171744	4073.7231	up	4073.7231	3600.1392
-16.50515	0.024295963	93013.086	down	-93013.09	-4895290.5
0.6550426	0.024993513	1.5746624	up	1.5746624	90883.89
-13.75823	0.025185674	13856.04	down	-13856.04	-15673.383
-13.64294	0.025370691	12791.854	down	-12791.85	-14469.542
-10.81263	0.02547326	1798.5686	down	-1798.569	-2033.5967
-10.7536	0.025527824	1726.4564	down	-1726.456	-1952.0211
-10.28215	0.025630502	1245.1852	down	-1245.185	-1407.5922
-9.393279	0.025814945	672.44806	down	-672.4481	-759.69415
-10.05848	0.025895737	1066.3583	down	-1066.358	-12614.292
-10.70735	0.026203861	1671.9869	down	-1671.987	-1890.4036
-9.846104	0.026781712	920.39136	down	-920.3914	-1040.1747
-9.672007	0.026887886	815.7632	down	-815.7632	-921.81604
-11.62794	0.02704956	3164.8997	down	-3164.9	-3579.2327
-11.05239	0.02710642	2123.7324	down	-2123.732	-2401.4321
-11.35168	0.027201256	2613.3342	down	-2613.334	-2955.285
-10.72455	0.027357979	1692.0427	down	-1692.043	-1913.0912
-10.03371	0.027414167	1048.206	down	-1048.206	-1184.7633
-9.99965	0.027440438	1023.7516	down	-1023.752	-1157.0996

-12.24901	0.027467487	4867.645	down	-4867.645	-5505.431
-9.711211	0.027518565	838.23517	down	-838.2352	-947.2376
-9.646583	0.027563078	801.51324	down	-801.5132	-905.6967
-9.82249	0.027581975	905.4491	down	-905.4491	-1023.2721
-10.17404	0.027652297	1155.2904	down	-1155.29	-1305.8995
-9.259206	0.027745854	612.77167	down	-612.7717	-692.18634
-9.401764	0.02791709	676.41455	down	-676.4146	-764.18115
-9.855497	0.028441766	926.4038	down	-926.4038	-11276.918
-11.05912	0.02904646	2133.6711	down	-2133.671	-2412.675
-9.715218	0.02909249	840.56616	down	-840.5662	-10110.91
10.007375	0.031232027	1029.2479	up	1029.2479	11227.518

Abund Diff (Log2)	Alignment Value	ChEBI ID	CompositeSpectrum	Mass
-18.17869			(391.28793, 16340.016)(392	392.2951
14.447212			(718.599, 1531.82)(719.598	719.6055
13.587301			(810.5079, 2796.5103)(811.	811.5144
13.1000805			(934.5643, 3082.9175)(935.	935.5716
16.013258			(822.43915, 24944.312)(823	823.4462
15.211804			(590.5232, 13872.777)(591.	591.5298
16.32327			(572.52795, 3386.4136)(573	537.5588
17.898687			(1506.1051, 829.38)(1507.1	753.5568
23.182467			(508.52103, 3217930.2)(509	509.528
15.492642			(794.4079, 21526.156)(795.	795.4147
16.249485			(612.69684, 14742.299)(613	613.7038
14.913971			(878.5015, 12617.505)(879.	879.5086
16.30963			(618.5355, 33105.984)(619.	619.5429
13.305708			(780.39325, 4319.403)(781.	781.4012
16.260786			(625.70654, 39599.11)(565.	566.6927
15.234604			(850.4705, 23252.906)(851.	851.4783
14.269907			(239.23674, 9783.122)(240.	240.2442
15.507067			(530.48047, 2384.6938)(531	495.5118
17.604147			(626.7126, 56446.402)(627.	567.6986
15.682883			(241.25255, 38201.016)(242	242.2597
12.057058			(797.39154, 2415.7976)(798	798.3992
13.601585			(808.4241, 5783.6025)(809.	809.4308
15.508161			(566.4789, 17863.572)(567.	567.4859
13.804244			(906.5325, 6764.4165)(907.	907.5388
15.422135			(646.55444, 7079.896)(647.	647.5615
18.447302			(632.55176, 175174.78)(633	633.5588
14.843368			(516.46387, 1563.6362)(517	481.4959
13.090727			(941.78296, 1573.7474)(942	942.7914
13.994268			(644.4874, 3041.311)(645.4	645.4982
12.692832			(828.7652, 668.44336)(792.	793.794
15.002667			(766.37646, 20441.887)(767	767.3841
13.887589			(633.50665, 4146.995)(634.	634.5134
11.725124			(881.48376, 2462.3774)(882	882.4914
12.835672			(706.7037, 1332.3586)(707.	707.7108
15.316587			(241.25273, 23733.406)(242	242.2601
12.531479			(724.3304, 2730.2988)(725.	725.3374
13.121777			(571.4953, 1846.8639)(572.	572.5035
14.549034			(738.34503, 16817.006)(739	739.353
12.176996			(505.4963, 2496.0798)(506.	506.5045
12.913131			(752.3635, 3525.7524)(753.	753.3713
17.505491			(507.51434, 103130.016)(50	508.5217
14.898531			(604.50793, 12258.867)(605	605.5148
13.924147			(672.5281, 1429.4241)(673.	673.5342
13.418156			(642.4071, 1130.4719)(643.	643.4132
13.993773			(895.7905, 1124.36)(896.79	896.7988
14.001427			(688.60046, 1276.5979)(689	689.6095

13.242032	(835.7707, 1240.078)(836.7	836.7786
13.717704	(696.29913, 1793.282)(697.	697.3067
12.950745	(807.74304, 1337.112)(808.	808.7509
13.782116	(710.31464, 9881.722)(711.	711.3218
12.423693	(477.5027, 4488.695)(478.5	478.5098
13.397118	(653.5351, 2806.3076)(654.	654.543
-14.113853	(1097.7836, 1215.135)(109	1098.7911
14.528566	(1097.784, 1234.1)(1098.78	1062.8143
13.601116	(1024.0537, 1503.7175)(10	1025.0608
21.169533	(1018.0504, 659275.6)(101	1019.0572
15.1130495	(1001.8049, 6280.0474)(10	1002.8115
15.446462	(629.6913, 9935.298)(630.6	630.6986
15.190352	(1040.0297, 9468.508)(104	1041.0367
13.020963	(1097.988, 1728.0325)(109	1098.9963
14.57087	(539.50287, 3018.9)(540.50	240.2442
13.7709255	(882.84125, 3709.8975)(88	883.8483
16.817593	(551.5037, 38803.242)(552.	552.5111
-12.471074	(614.499, 5810.3325)(615.5	615.5059
-10.941644	(940.6085, 1336.3586)(941.	941.6179
13.098574	(883.7776, 2406.0776)(884.	884.7848
13.219475	(653.49304, 1734.1824)(65	654.5008
13.411222	(726.67365, 2492.6763)(72	727.6817
12.512407	(451.45023, 2503.5837)(45	452.4582
-11.285672	(287.10825, 3992.33)(288.1	288.1173
-15.1770115	(290.90497, 1856.1719)(29	291.9122
-17.198414	(551.5038, 14632.885)(552.	552.5111
-12.133701	(1055.7761, 4075.3577)(10	1056.7855
-11.018249	(437.27725, 2324.3533)(43	438.2848
11.375064	(343.2338, 2480.7869)(344.	344.241
10.058337	(619.491, 1232.52)(620.494	620.4974
10.604065	(683.5102, 1545.8534)(684.	684.5189
11.1824875	(1155.0586, 910.93)(1156.0	548.0226
11.740564	(571.8481, 4850.8633)(572.	572.8572
11.431657	(1020.5393, 8242.671)(102	1021.5525
9.442136	(763.7514, 1161.9767)(764.	764.7597
10.910389	(862.6285, 1210.7667)(863.	863.6365
10.430017	(419.3043, 1839.3734)(420.	420.3119
10.622065	(630.20734, 1992.7032)(63	631.2144
9.739268	(592.6136, 1429.5533)(593.	593.6203
11.772378	(713.47363, 3146.8)(714.47	714.4809
9.671286	(607.5079, 1100.9033)(608.	608.515
11.116716	(511.87186, 5200.0034)(51	512.8693
13.122294	(558.50836, 637.3825)(522.	523.5431
11.43243	(789.61395, 2211.6833)(79	790.6112
12.012771	(794.5481, 2814.3232)(795.	795.5545
12.233984	(828.71106, 1346.6113)(82	829.7179
12.7368555	(684.4637, 561.22)(624.438	625.4464

12.504948	(825.4205, 3925.859)(826.4	826.4281
9.149434	(780.4028, 1992.63)(781.40	781.4095
11.989852	(853.45386, 2693.4448)(85	854.4591
-14.821398	(665.49664, 6485.576)(666.	666.5035
13.57152	(733.5816, 1921.435)(734.5	734.5882
15.638477	(593.5418, 7903.3667)(594.	594.5491
14.805527	(754.58185, 1383.6599)(75	753.5745
15.194512	(796.5645, 4072.4297)(797.	795.5572
-14.056743	(832.6198, 1425.1741)(833.	831.6166
-16.581503	(361.33246, 4904.488)(362.	360.324
-14.35105	(610.54645, 1930.6439)(61	609.5384
-13.29329	(978.84296, 1174.462)(979.	977.8417
-19.53423	(857.84143, 217741.38)(85	856.8291
16.336649	(361.33105, 3878.5122)(36	360.3239
13.777534	(723.50836, 1462.154)(724.	722.504
10.000782	(309.23477, 1623.8033)(31	308.2274
10.469365	(593.41815, 1242.6666)(27	277.227
10.552937	(529.4046, 1231.0533)(530.	528.3982
10.627539	(775.57355, 1948.1401)(77	774.5694
11.4587	(586.44366, 4390.143)(587.	585.4367
-10.253861	(319.21637, 2610.42)(320.2	318.2104
-11.612877	(589.4659, 3053.6165)(590.	588.4565
-11.322928	(543.40155, 2875.8867)(54	542.3964
-9.952732	(920.75507, 1103.2533)(92	919.7473
11.746806	(594.4964, 2140.8533)(595.	593.4894
-11.015094	(603.40936, 2243.79)(604.4	602.4018
12.997935	(560.4333, 11388.434)(561.	559.4262
-17.570782	(368.3729, 17773.307)(369.	367.3628
11.813837	(728.58057, 9520.267)(729.	727.5683
-22.222963	(186.22197, 764228.3)(187.	185.2139
16.471737	(202.21822, 28594.693)(20	201.2113
-13.936029	(447.35025, 57065.88)(448.	446.3449
-13.820731	(447.35165, 51714.34)(448.	446.3443
-10.989818	(872.7524, 1225.89)(873.74	871.7458
-10.930753	(433.33972, 5398.5864)(43	432.3353
-10.459014	(508.5825, 1118.8967)(509.	507.5766
-9.569275	(1697.6527, 1057.42)(1698.	1696.6396
-13.622771	(904.80566, 1509.876)(905.	903.8038
-10.884479	(816.66455, 1432.4332)(81	815.6512
-10.02261	(1011.699, 1115.6266)(101	1010.6949
-9.848335	(958.70294, 1139.0967)(95	957.6896
-11.805434	(261.15457, 7756.563)(262.	260.1458
-11.229679	(682.55176, 2029.85)(683.5	681.5471
-11.529081	(453.3689, 2153.96)(454.37	452.3585
-10.90169	(815.6065, 1696.3932)(816.	814.602
-10.210383	(759.69855, 2154.3767)(76	758.6929
-10.176297	(1042.7837, 1190.0366)(10	1041.7758

-12.42664	(731.612, 7137.719)(732.61	730.6056
-9.887583	(863.7835, 1236.44)(864.77	862.7744
-9.822885	(570.5477, 1313.0834)(571.	569.5366
-9.998974	(389.25525, 1727.9434)(39(	388.247
-10.350828	(849.6731, 2230.5198)(850.	848.6615
-9.435017	(750.32007, 1152.0599)(75:	749.3153
-9.577771	(896.861, 1097.23)(897.848	895.8587
-13.461085	(820.7433, 1326.2161)(821.	819.7402
-11.236418	(814.68915, 5866.6626)(81!	813.6815
-13.303625	(794.7292, 1428.0519)(795.	793.7219
13.454751	(765.63916, 1181.9099)(76(	764.6341

Retention Time	HMP ID	KEGG ID	LMP ID	Ionization
10.1814995				-
9.690249			LMGP02040002	-
6.69825			LMGP02010961	-
10.32				-
9.345625		C15732		-
9.67875				-
9.947374				-
6.6997495			LMGP02010329	-
9.689125				-
9.01925		C15705		-
7.652				-
9.887375			LMGP01030017	-
8.5130005		C18138		-
9.0195				-
7.6509995				-
9.62225		C15729		-
10.410376	HMDB0155	C00517	LMFA06000088	-
9.529125				-
7.6485				-
10.410126			LMFA05000010	-
9.020625				-
9.34525		C15704		-
9.679249				-
10.119625		C05306		-
9.68425				-
8.513376				-
9.373624				-
10.436375				-
9.685876			LMGP02020039	-
10.519501				-
8.648625		C03796		-
7.8888755			LMGL02010196	-
9.886624			LMST01080090	-
7.659375		C15244		-
7.887875			LMFA05000010	-
8.226375				-
7.9888754				-
8.226999				-
7.8872504			LMFA01020322	-
8.647875				-
7.88775			LMFA01020318	-
9.677375				-
9.6826			LMGP02020102	-
9.6798		C16998		-
5.2937994		C14438		-
9.6846				-

10.0204	C15798		-
7.7398005	C12044	LMPK05000005	-
10.408999		LMST01010135	-
7.7454996	C19247		-
10.409625			-
8.578875	C05811		-
10.771501			-
10.766999			-
9.682			-
9.681625			-
10.81375		LMGL03012585	-
7.64125		LMFA05000036	-
9.677375		LMFA07010023	-
9.676624		LMST03020221	-
7.8883758	HMDB0155	C00517	LMFA06000088	-
9.727125			-
6.345625			-
7.889375			-
6.7009997			-
7.889125		LMGL03010272	-
8.306749		LMGP10030037	-
7.6369996	C18965		-
9.174375		LMFA01020314	-
5.211	C11769		-
5.2922			-
6.2144			-
10.81925		LMFA01170127	-
3.9363334		LMFA01050016	-
5.32		LMFA03010086	-
7.8863335	C14308		-
9.488667		LMFA01060043	-
9.683			-
5.3103333	C18779		-
9.689	C18059		-
10.410666		LMFA01020350	-
7.704666		LMSP0501AB14	-
9.8186655		LMST03020391	-
6.5606666			-
10.400001	C19224		-
7.9236665		LMGP04010195	-
9.676999			-
9.702	C11040		-
9.811251			-
7.778667		LMST01150011	-
7.926	C11698		-
7.69975	C01060		-
9.6797495			-

9.345				-
8.859125		C14059		-
9.620875		C17042		-
7.8868756			LMGP10020031	-
9.444		C15013		-
5.29775		C07036		-
6.1599994				+
8.234601			LMGP06020042	+
8.1264			LMGP03010245	+
4.4812				+
8.2306			LMGL02010022	+
10.4326			LMGL03011675	+
10.624375			LMGL03010013	+
4.3891997				+
6.3623996			LMGP10030023	+
10.086333		C15033		+
0.92333335				+
4.147333	HMDB0681(	C13425		+
8.155				+
0.9253333		C16505		+
10.634		C06998		+
6.696333	HMDB07153			+
0.928	HMDB0192(	D00848		+
10.632333			LMGP02010202	+
4.1056666			LMGL02010311	+
0.91899997				+
11.537999		C07881		+
5.0903997				+
8.087001			LMGP02020053	+
0.8116		C02277	LMFA05000001	+
0.8846251			LMFA05000154	+
10.760333	HMDB02163			+
10.505	HMDB02163			+
6.845			LMGL03010012	+
11.319333				+
10.271		C14708		+
10.622334				+
10.643				+
5.2023335	HMDB0497{	C01190		+
8.436667			LMST03020495	+
9.744334		C04150		+
4.858667				+
4.712667		C05813		+
5.237				+
8.137666		C16248		+
9.497333	HMDB10376			+
4.7036667	HMDB10561			+

7.904	C10385		+
10.317334		LMFA01020362	+
6.331		LMSP02020019	+
10.967			+
8.302001		LMGL03010037	+
7.682667		LMPK12140071	+
10.836334			+
10.134199		LMGL03010018	+
8.735333		LMSP0501AA23	+
10.106199	HMDB10412		+
8.7364		LMFA01020037	+